Spatiotemporal development of cuticular ridges on the leaf surfaces of *Hevea brasiliensis* alters insect attachment

Venkata A. Surapaneni[*1], Georg Bold[2], Thomas Speck[3], Marc Thielen[4]*

[1,2,3,4]*Plant Biomechanics Group, Botanic Garden, Faculty of Biology, University of Freiburg, Schänzlestrasse 1, 79104 Freiburg, Germany.*

[1,2,3,4]*FIT, Freiburg Center for Interactive Materials and Bioinspired Technologies, Georges-Köhler-Allee 105, 79110 Freiburg, Germany.*

[1,2,3,4]*FMF, Freiburg Materials Research Center, Stefan-Meier-Strasse 21, 79104 Freiburg, Germany.*

[3]*Cluster of Excellence livMatS@ FIT- Freiburg Center for Interactive Materials and Bioinspired Technologies, University of Freiburg, Georges-Köhler-Allee 105, 79110 Freiburg, Germany.*

[*1]***amarnadh.sv@bio.uni-freiburg.de*** *(corresponding author)*

[2]*georg.bold@biologie.uni-freiburg.de*

[3]*thomas.speck@biologie.uni-freiburg.de*

[4]*marc.thielen@biologie.uni-freiburg.de*

Abstract

Cuticular ridges on plant surfaces can control insect adhesion, wetting behaviour and might also offer stability to underlying cells during growth. Yet, the influence of ontogenetic changes in the morphology of such surface microstructures on interactions of insects with plant organs has been largely neglected. In this study, we present spatial and temporal patterns in cuticular ridge development on the leaf surfaces of the model plant, *Hevea brasiliensis*. Through confocal laser scanning microscopy of polymer replicas of the leaves, we identified an acropetally directed progression of ridges during the ontogeny of *Hevea brasiliensis* leaf surfaces. Using Colorado potato beetles *(Leptinotarsa decemlineata)* as model insect species, we show that the changing dimensions of cuticular ridges on plant leaves during ontogeny have a significant impact on insect traction forces and act as an effective indirect defence mechanism. The traction forces of walking insects were significantly lower on mature leaf surfaces compared to young leaf surfaces, and the measured walking traction forces showed a strong negative correlation with the dimensions of cuticular ridges.

Keywords: cuticle, fold, ridge, *Hevea brasiliensis*, ontogeny, plant defence, replica, adhesion, friction, plant-insect interactions

Introduction

Plant-animal interactions have a strong influence on life on earth and is crucial for species distribution, crop yield and food security. Insects constitute a major portion of these interactions and can be either detrimental to plant life as consumers of plant organs or favourable by acting as pollinators or protectors or even as a prey. They can also stay neutral by using plants as a place to rest or hide. The interactions between plants and herbivores can be highly complex and dynamic due to growth-induced changes in both herbivore and plant traits. The ontogeny of plant defence mechanisms varies among different plant species depending upon the type of geographical region, defence mechanism or herbivore. In addition, it could also correlate with the ontogenetic changes occurring in the herbivore [1, 2]. In addition, the trajectories of defence mechanisms may vary between organs (e.g, leaf) and whole-plant ontogeny [3]. While chemical resistance of the plants and digestive ability of the herbivores has been the main subject of interest to assess plant defensive behaviour, understanding mechanisms at other levels of interactions [4] is also important to determine the levels and efficiency of plant defence. For instance, the insect herbivory or mutualism is dependent upon how well the insects are able to hold on to or walk over the plant surfaces. Evolution of complex attachment systems of insects as an adaptation to plant surfaces [5, 6] shows the significance of the mechanical interactions between these attachment structures and the plant surfaces. Nevertheless, the ontogenetic changes in plant cuticular microstructures as a mechanism of structural defence against insect herbivores has not been studied in detail yet [7, 8, 9]. Nano- to micro-scale morphological changes due to growth at the interface – the plant cuticle – can alter insect walking friction forces and influence the way insects interact with plant organs, which is the focus of this study.

The plant cuticle is a continuous extracellular membrane covering the surfaces of most above ground organs of land plants. As an interface between plant epidermal cells and the surrounding environment, it incorporates a highly multifunctional structure necessary for plant survival. The cuticle serves as a transpiration barrier protecting the underlying tissues against water loss and regulates gas exchange along with other functions such as UV light reflection, mechanical integrity, control of water repellence, particle adhesion and animal interactions [10, 11, 12]. The mesoscale morphology on the peripheral side of the cuticle is highly diverse among different plant species and includes hairs, branched or unbranched trichomes, cuticular ridges and valleys (also referred to as wrinkles, or striations), and epicuticular waxes [13, 14]. The cuticle structure is dynamic and thus changes continuously during the ontogeny of a plant due to new material deposition and growth of the underlying epidermis [15]. These structures in addition to different

cell shapes and surface chemistry influence abiotic interactions with water and light [16] and biotic interactions with pollinators, herbivores and prey on plant surfaces [17].

Insects' ability to adhere can be reduced on plant surfaces with epicuticular waxes, cuticular ridges and trichomes as compared to smooth surfaces [6, 18, 19, 20, 21, 22, 23]. Cuticular ridges are of particular interest in a biomimetic point of view as they are mechanically relatively robust compared to wax-like structures [22, 24] and also because of ease of their production [25]. Artificial periodic and randomly oriented ridges were shown to reduce insect attachment with lowest walking forces occurring at ridge dimensions in the critical roughness range of 0.3 to 3 µm [26, 27]. In fact, rough surfaces with different morphologies and surface chemistry [22, 23, 24, 28, 29, 30, 31] showed reduced insect adhesion forces in this roughness range. It is then interesting to know whether the cuticular structures on plant leaves also display this critical roughness and at which ontogenetic stage do they achieve it.

The goal of this study is to understand: 1. at what point during the growth of the leaves do cuticular ridges appear? 2. how does the ridge morphology changes during growth? and 3. how these growth-induced changes of plant surfaces affect insect walking behaviour? To study the ontogenetic development of ridges on leaf cuticles and the corresponding changes in insect walking forces, we chose *Hevea brasiliensis* as a model plant. Originally from the Amazon basin, now grown widely in South and Southeast Asia, it is a tropical plant species with tri-foliated leaves and is a prime source of natural rubber [32]. Rao, 1963 [33] first reported the presence of cuticular ridges on the adaxial side and reticulate structures on the abaxial side of *H. brasiliensis* leaves. Here, we make use of polymer leaf replicas to study the morphological changes of these cuticular ridges during ontogeny. The polymer replication of leaf surfaces provides a great practical advantage in studying the variations in surface microstructures, which is otherwise difficult because of slowly dehydrating leaf samples [12]. The replicas are useful in carrying out repeatable and long-term studies, especially for young leaf samples that have translucent cuticles, and can be stored for further experiments. In particular, the confounding variables associated with surface chemistry and even chemical changes associated with defensive mechanisms that might occur during the experiments can be eliminated or controlled. For analysis of insect walking friction forces, we selected the Colorado potato beetle (*Leptinotarsa decemlineata*) having hairy attachment systems as a model species owing to the availability and ease of experimentation. More importantly, the attachment structures of Colorado potato beetles are similar to that of other relevant insects for example, Mupli beetle (*Luprops tristis,* a common herbivore of *H. brasiliensis* leaves) [5]. The selection of these plant and insect model species in

this study provides a general insight on how beetles' walking abilities (measured as traction forces) vary corresponding to the ontogenetic growth induced changes in the plant cuticular structures. Through confocal microscopy observations and traction force experiments, we show that the changing dimensions of cuticular ridges on plant leaves during ontogeny have a significant impact on insect walking behaviour.

Results

Ontogeny and cuticular ridge development

The leaves of the *Hevea brasiliensis* tree (Fig. 1) studied reached growth stage S1 in 11 to 15 days from the formation of bud. The acropetally directed transition of the leaf surfaces in the form of striking colour changes occurred immediately after S1 during the transition to S2 in 1 to 3 days. Once the transition (S2 to S3, 1 day) was complete, the leaves continued growth exponentially (Supplementary Fig. S1) until reaching S4 for 4 to 6 days. Thereafter, no significant growth of the leaves was recorded. The changes in the colour of the leaves with growth stages and the CLSM observations on each stage are shown in Fig. 2.

After ca. 60 days from bud formation, the leaves (S5) showed apparently reduced hydrophobic behaviour and had dust particles accumulated on their surfaces which was not observed on leaves at earlier growth stages. Throughout all the stages, the colour variation of the leaves was visually evident with dark brown colour (S1 and S2A) during the initial stages of leaves, gradually changing to pale green with a colour gradient moving from the base of the leaves towards the apex (S2B and S3) before finally shifting to dark green (S5). Interestingly, the colour variations of the leaves coincided with the cuticular ridge formation and development on the leaf surfaces.

The CLSM measurements of replica surfaces (Fig. 2, Supplementary Fig. S2) and the results from initial experiments showed that until stage S1, the leaf surfaces of *H. brasiliensis* were composed of smooth cells free of ridges. Immediately after, the ridges started developing rapidly during S2 and S3 progressing acropetally from base to the apex of the leaves. At stage S2, the area towards the apex (S2A) contained smooth cells similar to those of S1. At the stages S2B and S3, high aspect ratio and dense cuticular ridges covered the surfaces (cf. Table 1). This resulted in firm sticking of the original leaf material to all epoxy negative replicas (moulds) of these stages, requiring KOH treatment in order to remove the plant material from the surfaces. Yet, thin residues of plant material remained fused rather uniformly to the epoxy moulds (Fig. 3) even after KOH treatment and ultrasonication, making it difficult to quantify the morphology of ridges on leaf surfaces at these stages precisely as can be seen in Supplementary Fig. S3, which shows

SEM images of an epoxy replica with attached plant material. This also influences the positive replicas, which are free of plant residues, but only mirror the negative moulds contaminated by plant residues, resulting in a significant reduction of the real aspect ratio of the ridges (Fig. 4 (a, b), see also Table 1). For the morphometric comparison we were able to use the data from tiny spots (only 1 to 14 spots with area around 2500 to 6400 μm^2) where the epoxy moulds were not tainted with plant residues and the real high aspect ratios could be measured. The roughness parameters of these spots are included in Table 1 (data not in parenthesis) and Fig. 5. The roughness parameters of positive replicas from the large tainted negatives of stage S2B and of stage S3 are also given in Table 1 (data in parenthesis) and Fig. 5. As the tiny untainted spots of the positive replicas were too small for mechanical testing, we could only perform traction force measurements of stages S2B and S3 on positive replicas from the large tainted negative moulds, being well aware that these data – because of the markedly reduced aspect ratio of the ridges – probably overestimate the real traction forces on surfaces of these stages (Fig. 6). The removal of the plant material from the epoxy negative was much easier in regions closer to the base in stages S2B and S3 (Fig. 3). Our observations showed developed ridges in these regions with a morphology very similar to that of adult stages. Figure 4 (c) shows such a region on one of the replicas at S3. After stage S3, the ridges developed in a labyrinth-type arrangement over the entire area of the leaves with reduced height and increased spacing until S4 where the leaf growth stopped. At stage S5, the morphology of the ridges remained similar to that of S4. These observations reveal three distinct levels of microstructural surface morphology on the adaxial side of the leaves of *H. brasiliensis*: (1) surfaces with smooth cellular structure with no ridges from bud appearance until stages S1 and S2A, (2) high aspect ratio ridges at stages S2B and S3, and (3) labyrinth-type arrangement of developed ridges at stages S4 and S5.

Ridge dimensions

Roughness values Rc, Ra, Rsk and Rsm of leaf replicas were compared within different leaf stages. The variations in roughness are shown as ridge aspect ratio (AR = Rc/Rsm) versus leaf stage in Fig. 5. The roughness values of the replicas of leaves from all the stages compared with glass and its replica (i.e. flat PDMS) showed significant differences *(ANOVA type III on GLMM, $p < 0.001$, n=369).* The median values of these roughness parameters on five replicates of glass, flat PDMS and leaf replica surfaces are given in Table 1. For reasons discussed above for states S2B and S3, the roughness values for untainted replicas and replicas from tainted moulds are given.

The variations in roughness were compared using the arithmetic average of the roughness (Ra) and mean aspect ratio of the ridges (AR=Rc/Rsm). The aspect ratio and Ra of the ridges did not vary between glass and flat PDMS *(AR: $p = 0.971$, Ra: $p = 0.446$, $n=50$)* but varied significantly between flat PDMS and S1 leaves *($p < 0.001$, $n=50$).* The AR and Ra values did not change significantly from S1 to S2A leaf surfaces *(AR: $p = 0.894$, Ra: $p = 0.644$, $n=50$)* as the apical part of the leaves at S2 had not yet developed ridged morphologies on their epidermal cells. The region towards the base of the leaf however had already developed ridges. The roughness parameters of the untainted spots on the replicas of S2B were significantly higher *(AR: $p < 0.001$, Ra: $p < 0.001$, n, S2A=50, n, S2B=36)* compared to S2A. There were no significant differences in the roughness parameters between S2B and S3 *(AR: $p = 0.619$, Ra: $p = 0.314$, n, S2B=36, n, S3=33)*. From the stages S3 to S4, no significant differences in the Ra values were found (*$p = 0.903$, n, S3=33, n, S4=50)*, but the aspect ratio of the ridges decreased significantly (*$p = 0.007$, n, S3=33, n, S4=50).* In spite of large age difference, there were no significant differences in the AR and Ra values between S4 and S5 *(AR: $p = 0.907$, Ra: $p = 0.968$, $n=50$)* showing that the development of the ridges ceases during stage S4. However, a relatively large difference in Rsk value can be found between these stages (Table 1). A higher value of skewness generally indicates the presence of sharper ridges with larger valley size and a lower value indicates the presence of blunt ridges with smaller valley size. The skewness parameter changed from 0.215 for S4 leaves to 0.035 for S5 leaves (Table 1) with almost constant spacing between the ridges thus suggesting relatively blunt ridges on S5 leaves. The negative skewness values of the ridges for stages S2B and S3 indicate dense arrangement of ridges with lesser amount of valleys. The variation of Ra and AR within replicates (leaf samples) in each stage was less than 15% compared to the residual variance. At least three out of five replicates in each stage showed no significant spatial variation in Ra and AR of the ridges in the direction perpendicular to the midrib and at least four out of five replicates showed no significant variation in Ra and AR of the ridges in the direction parallel to the midrib. No significant effect of leaf area on the roughness parameters was observed.

Insect traction forces

Our experiments showed a significant effect of ontogenetic changes in leaf surface structure on insect traction forces. The maximum insect traction forces on the PDMS replicas of leaves at all stages (and on the flat glass PDMS replica) differed significantly from those on glass *(ANOVA type III on GLMM, $p < 0.001$, $n=240$).* We have excluded the results of insect traction forces on the S2B and S3 leaf replicas from the statistical analysis for above mentioned reasons. Figure 6

shows the variation in the mean traction forces of insects of glass, flat PDMS and leaf replica surfaces. Our experiments showed that the traction forces on flat PDMS glass replica surfaces were much lower as compared to glass surfaces *($p < 0.001$, $n=40$)* showing the effect of surface chemistry on insect adhesion. Compared to the flat PDMS surfaces the replicas of leaves at S1 *($p = 0.996$, $n=40$)* and S2A *($p = 0.963$, $n=40$)* did not differ significantly in insect traction forces. Even though the dimensions of the ridges were influenced by the plant remnants for S2B (replicas from tainted moulds), the traction forces showed a decrease in magnitude compared to those on the surfaces towards the apex (S2A). In reality, the insect traction forces could be even lower on the leaves at stages S2B and S3 as compared to those obtained in our experiments or be comparable to the traction forces on leaves at stage S4 owing to the high aspect ratio of the cuticular ridges found for patches without plant residues at the transition stages. The traction forces on the adult leaf replicas (S4 and S5) were significantly lower *($p < 0.001$)* compared to those on young leaves (S1 and S2A). The mean traction forces at stage S5 increased significantly *($p = 0.049$, $n=40$)* compared to the forces at stage S4. Analysis of random effects showed relatively lower influence of replicates i.e., variation within leaves in each stage (4.2%, variance: 0.003, residual variance: 0.038) compared to that from beetles (27.4%, variance: 0.014, residual variance: 0.038) and the differences in traction forces within replicates in each stage were not significant. During the experiments, the interaction of beetles with the protruding veins has been unavoidable. Nonetheless, these structures do not seem to effect the reduction of traction forces during leaf growth. The log transformed mean of traction force and mean aspect ratio (AR) values taken over replicates showed a strong association *(Pearson's product-moment correlation, $R = -0.91$, $df = 28$, $p < 1.9e-12$)* (Supplementary Fig. S4). The association between log transformed values of traction forces was also strong compared to Rc and Ra (both, $R = -0.90$, $df = 28$, $p < 1.0e-11$). However, no correlation was found between log transformed values of traction forces and Rsm ($R = 0.28$, $df = 28$, $p = 0.18$).

Discussion

In this study, the definition of leaf growth stages of *Hevea brasiliensis* was based on a combination of visual colour changes on the adaxial side of the leaves (S1, S2 and S3) and growth (S4 and S5). Initial screening using confocal laser scanning microscopy helped to verify the segregation of the stages S1, S2 and S3 based on the colour differences as they clearly corresponded to the drastic changes in the surface microstructure. This differs from the definition of leaf growth stages for the same species in earlier studies, which were based on macroscale morphological parameters or physiological data. Based on morphology for example, Dijkman,

1951 [34] discerned four leaf growth stages A, B, C and D corresponding to bud burst, young, fully expanded and mature states respectively. The stages A to C act as sink leaves with almost no lignin and vary physiologically for example in chlorophyll amount, cyanogenic capacity etc. [35, 36] and stage D leaves are mature source leaves with a high amount of lignin [37, 38]. As our work is aimed at understanding the effect of changes in the morphology of surface microstructures on insect walking forces we based our classification on these microstructures, which, nevertheless are reflected to a large extent also by macroscopically visible features (i.e. colour). These microscopic changes on the leaf surfaces however did not match with the previously defined stages by Dijkman, 1951 [34]. The growth stages S1, S4 and S5 defined in this study correspond to the stages B, C and D respectively. From this comparison, the leaves from stages A to B contain smooth epidermal cells and the cuticular ridges develop completely until stage C. The ridge morphology at stage D remains similar to that of stage C. In addition to these, our definition includes intermediate stages S2A, S2B and S3 between B and C, where sudden transition from smooth to dense ridge morphology occurred on the leaf surfaces simultaneously with the exponential growth of the leaves. Chemical changes were earlier attributed for colour variations of *H. brasiliensis* leaves. The shiny brown colour during the initial stages of *H. brasiliensis* leaves is due to the presence of higher amount anthocyanin pigments compared to the adult stages of the leaves [39]. The changes in thickness of the leaf cuticle along with the cell wall material might also contribute to the variation in colour. Whether the colour affecting chemical changes also progress simultaneously with the cuticle development is yet to be understood.

Rapid changes in the cuticular morphology on the adaxial leaf surfaces of *H. brasiliensis* during the transition stages occurred directionally with ridges progressing acropetally from base to apex from stages S1 to S3. Such ontogenetic development of ridges was also observed on *Arabidopsis thaliana* sepals [40] where the ridges progressed basipetally from tip to base of the sepals. On *A. thaliana* sepals, the ridge progression correlated with the reduced growth rate and termination of cell division of the underlying epidermal cells [40], which seems a probable cause also in case of *H. brasiliensis* leaves. In addition to the acropetally progressing formation of ridges during the ontogeny of *H. brasiliensis* leaves a second process is superimposed. At the transition stages S2B and S3, stretching and thickening of the originally high aspect ratio ridges starts from the leave base eventually leading to the typical ridge pattern found in the later stages (Fig. 2 and Fig. 3). In these stages, we did not observe significant spatial variation of ridge morphology over the leaf area except in these basal regions. This suggests that both ridge formation and development

processes on *H. brasiliensis* leaves are not gradual but occur sequentially, possibly a result of polarity in cell maturation and growth. Further work is needed to confirm this hypothesis.

Martens, 1933 [41] proposed that the formation of ridges is due to over secretion of cuticle over the growing epidermal cells. Recently, a mathematical model proposed the formation of ridges to be a result of mechanical buckling of the cuticle due to compressive stresses arising from mismatch in epidermal cell expansion and cuticle production [42]. Once formed, the morphology of ridges is expected to change with growth. This will be interesting as it hints at the timing when cuticle production outpaces the underlying epidermal cell growth or vice versa. It is intuitive that when the rate of cuticle production reduces, the cuticle is stretched due to growing underlying epidermal cells. Our measurements on the surfaces of *H. brasiliensis* leaves show that the ridge development stops at stage S4 where the leaves attain maximum growth and thereafter no significant changes in the ridge aspect ratio occurs until stage S5. This shows that the ridge development occurs only simultaneously with growth on *H. brasiliensis* leaves, with sudden formation of ridges in transition stages (S2A and S3) and further development until leaf growth ceases. Changes in the amount and chemistry of cuticular waxes also occur during the growth of leaves and may lead to changes in the hydrophobic behaviour of the leaf surfaces [43, 44, 45]. When the hydrophobicity of the leaf surfaces is reduced with age, damage of superficial waxes [46] can also occur due to rain water, dust etc. under field conditions thus changing the morphology of the cuticular surface. Our model species was grown in a tropical greenhouse and we believe that in addition to possible additional cuticular wax deposition, this could be a reason why the leaf replica surfaces at stage S5 showed reduced skewness parameter compared to those at stage S4.

While *Leptinotarsa decemlineata* is a pest specific to potato plants, the attachment systems [5] are comparable to other related harmful pests. Relating the interaction abilities of insects on *H. brasiliensis* leaves for example, leaf eating *Adoretus compressus* (Coleoptera) [47] or litter beetle *Luprops tristis* (Coleoptera) [48, 49] could help in understanding plant-insect interactions especially with respect to ontogeny. Litter beetle *Luprops tristis* is found to have minimum preference to matured leaves of rubber trees, but feed largely on the premature leaf litter [48]. This is because the leaves of *H. brasiliensis* were shown to employ cyanogenic chemical defences during early growth stages and lignification in adult stages particularly efficient against herbivore and pathogen attack respectively [38, 39, 50]. However, insect herbivory on young developing leaves seems to be a global phenomenon. During early stages, plants contain defensive secondary chemicals but high nutrition value which decrease in amount with growth.

Whereas in the later stages, physical traits such as leaf toughness, non-glandular trichomes and indirect defences like extra floral nectaries attracting predators eating pest insects were found to dominate [2, 51]. Nevertheless, the physical changes occurring in the cuticular microstructures during growth as a measure of indirect defence have been neglected. Assuming resource allocation and root to shoot ratio as a defining criteria for whole-plant defence, Boege and Marquis, 2005 [1] proposed that the plant defence is lower during young seedling stage, gradually increases with growth and finally decreases during over-mature stages. In line with this theory, our study also showed this pattern on *H. brasiliensis* leaves with high insect traction forces during young leaf stages, which significantly decrease with growth until full expansion and then increase significantly at much later (over-mature) growth stages. The fact that the variables of surface chemistry have been eliminated in our study implies that the dimensional changes in micro-scale plant surface structures alone can influence how insects can forage and feed on plant organs. We suppose that similar changes in physical defence traits also occur on other plant species having cuticular structuring. In addition to chemical defences and internal structural changes like cell wall hardening and lignification that stiffen the plant structure, we argue that the changes in cuticular patterning is a dominating indirect structural response strategy of plants with insect herbivores.

The comparably smooth surfaces of the epidermal cells of the leaves at early ontogenetic stages provide maximum contact area (Fig. 7 (d)) for the hairy attachment systems of beetles (Fig. 7 (a, b, c)) and therefore higher traction forces. On the microscale wrinkled surfaces however, the possible contact area is reduced (Fig. 7 (e)) leading to reduced forces [22, 23, 24]. Earlier studies found that there exists a critical roughness of surfaces with asperity size close to 0.3 to 3 µm at which insects fail to maintain proper attachment [5, 28, 29, 30, 31, 52]. Our data prove, that the dimensions of the cuticular ridges on the adult leaves of *H. brasiliensis* also fall in this critical roughness regime which explains the reduction of insect adhesion forces. This knowledge is important in a biomimetic perspective since the small changes in the structural parameters of plant surfaces can show how insects behave on these surfaces and provide a way to the development of artificial insect repellent surfaces [27]. It also has great potential in agriculture as new genetic [53] and technical tools become available for solutions to pest or pollinator management.

In summary, the CLSM measurements on the PDMS replicas of *H. brasiliensis leaves* showed how microstructural morphology of the leaf cuticle changes spatially and temporally during ontogeny. Insect adhesion was found to be greatly influenced by the growth-induced

morphological changes in leaf cuticular morphology and this signifies how plant indirect structural defences vary during ontogeny. The changes in insect walking forces were compared with the dimensional parameters of cuticular structures and the forces were found to have strong correlation with roughness parameters. Our results provide valuable insights for technical and genetic agricultural solutions for pest management and is also beneficial for biomimetics in developing chemical free insect resistant surfaces.

Materials and Methods

Leaf collection

Fresh leaves were collected for experiments from the model species, *Hevea brasiliensis* (tree > 10 m height) cultivated in the tropical greenhouse of the Botanic Garden of the University of Freiburg (avg. temperature = 28° C, avg. humidity = 57%). The leaves were monitored during growth from bud burst to adult stages, and fresh leaves for the experiments were cut at five defined ontogenetic stages. The determination of leaf growth stages was based on a combination of visual appearances of the adaxial leaf surfaces and leaf growth after preliminary trial experiments under a confocal laser scanning microscope, the details of which are given in the Supplementary Table 1. The leaves at *'stage 1'* (S1, age: 13 ± 2 days after bud burst) were shiny brown in colour and did not have microscale ridges on their surfaces. These leaves were just about to transform from a smooth cellular surface to a ridged surface evident from the appearance of pale green colour at the very base of the leaves. The *'stage 2'* leaves (S2, age: 15 ± 3 days) had half transformed surfaces with ridges covering 40-60% of the leaf surface starting from the base of the leaves. These leaves were again divided as *'stage 2A'* (S2A) and *'stage 2B'* (S2B). S2A refers to the area towards the apex having no ridges and still a brown coloured surface, and S2B, the area towards the leaf base with ridges and a pale green coloured surface. The *'stage 3'* leaves (S3, age: 16 ± 3 days) had ridges on the entire area of the leaf surface. Hereafter, we refer S2 and S3 stages as the transition stages. The growth of the leaves as estimated from the length of the midrib (Supplementary Fig. S1) ceased at *'stage 4'* (S4, age: 21 ± 4 days). For *'Stage 5'* (S5), leaves with an age greater than 60 days have been chosen. Once the leaves were cut, the cut ends were immediately sealed with petroleum jelly (Vaseline) in order to prevent dehydration before the experiments. The replication process of the leaf surfaces was started within 10 min after the leaves were cut. Before replication, the leaves were cleaned gently using deionized water and carefully dried using compressed air.

Surface replication

For leaf surface replication, an Epoxy-PDMS replication method as described in Kumar et al., 2018 [54] was used, except that entire leaf laminas (min. leaf lamina area = 1168 mm^2, max. leaf lamina area = 14383 mm^2) were replicated in our study. The leaves were first attached to a clean flat plate using double sided adhesive tape (Tesa SE, Norderstedt, Germany) with the adaxial side of the leaves facing upwards. The perimeter of the leaf was framed with poly-vinyl siloxane (PVS, President Light Body, ColteneWhaledent, Altstätten, Switzerland) a common imprinting material for dentistry having fast polymerization times of around 10 min, in order to create a casting mould.

For negative replica, a two component epoxy resin (Epoxy Resin L & Hardener S, Toolcraft, Conrad Electronic SE, Hirschau, Germany; resin to hardener mixing ratio of 10:4.8) was uniformly mixed in a plastic cup for about 5 min, using a glass rod. After degassing in a vacuum chamber for 15 - 20 min to remove trapped air bubbles, the epoxy resin was carefully poured onto the leaf surface. Following overnight curing (~15 hours) of the resin at room temperature, the leaves were carefully peeled off from these now cured epoxy negative moulds. If necessary, potassium hydroxide solution (KOH, ≥ 85%, p.a., Carl Roth GmbH&Co. KG, Karlsruhe, Germany; concentration of 60 g/100 ml) was used to separate the leaves from the epoxy moulds, the reasons for which are discussed later. In this case, the epoxy mould with leaf remnants sticking to it was placed in a KOH solution at 60±3°C with a magnetic stirrer running at 450 ± 25 r.p.m. for 20 h, followed by ultrasonication (in deionized water) for 10–15 min.

For positive replica, a two-component polydimethylsiloxane (PDMS) elastomer (Bluesil ESA 7250 A & B kit, Bluestar Silicones GmbH, Leverkusen, Germany; weight ratio of 10:1) was used. A drop of red coloured dye (Holcosil LSR Red, Holland Colours Europe BV, Apeldoorn, Netherlands) was added to reduce transparency and thus to ease microscopy observations. The components were uniformly mixed in a plastic cup for about 5 min and degassed until the air bubbles in the mixture were removed. The mixture was then slowly poured onto the negative moulds and kept in a vacuum chamber for 1 h to remove any remaining air entrapped around the sample. The air-free mixture was then placed in an oven at 60°C for 4 h for curing. The cured replicas were then gently peeled off and cleaned in isopropyl alcohol (≥ 99.95%, Carl Roth GmbH & Co. KG, Karlsruhe, Germany) in an ultrasonicator for 10 min, followed by drying. A total of five leaves within each ontogenetic leaf stage were replicated. For comparisons, five clean glass slides were also replicated and henceforth we term the replicas of glass as 'flat PDMS'. The efficiency of replication for young and adult *H. brasiliensis* leaves was quantified

in Kumar et al., 2018 [54] to which we refer for further details on the process and the details on the efficiency of replication.

Surface characterization

The replicas of fresh leaf samples were characterized using a confocal laser scanning microscope (CLSM, Olympus LEXT OLS4000, 405 nm laser, Olympus Corporation, Tokyo, Japan). On each leaf replica a total of 10 randomly selected spots of 65 x 65 µm size on both sides of the midrib were recorded at 4320-fold (50x objective) magnification. A commercial surface analysis software (Mountains Map Premium version 7.4, Digital Surf SARL, Besançon, France) was used to analyse the measurements from CLSM. On each spot, after a median noise filter was applied, zig-zag profile lines of at least 200 µm in length were taken on the topographic layer. A standard Gaussian filter was applied on the profiles to separate waviness and roughness (2.5 µm for glass, flat PDMS, S1, S2, S3; 8 µm for S4 and S5). Line roughness parameters Rc (mean height), Ra (arithmetic average of the roughness), Rsm (mean spacing) and Rsk (Skewness) were then calculated from the roughness profiles [55]. For ease of comparison, the mean aspect ratio (AR=Rc/Rsm) was defined to characterize and compare the changes in ridge dimensions and the effect on insect adhesion. The Fiji image processing package, running Image J version 1.51u [56] was used for leaf area measurements.

Scanning electron microscopy (SEM) observations of replica samples and beetle tarsal attachment systems were carried out using a Leo 435 VP, Leica, Wiesbaden, Germany, at an accelerating voltage of 15 kV. Prior to SEM visualization, dead beetles were dehydrated in a graded methanol series (50%, 70%, 100% methanol each for 24 hours) before critical point drying (LPD 030, Bal-Tec) in ethanol [57]. The dried specimen along with the leaf replicas were immediately transferred to a gold sputter coater (Cressington Sputter Coater, 108 auto) for 15-20 nm gold coating before examination in SEM.

Insect species and traction experiments

Female Colorado potato beetles (*Leptinotarsa decemlineata*, Coleoptera: Chrysomelidae) were used as model insect species (with hairy tarsal attachment system) for traction experiments. All the beetles were collected from a potato field (organically farmed) in Kirchzarten area near Freiburg, Germany and kept in a terrarium. The beetles were fed with potato leaves and the lighting conditions were fixed at a day-night regime of 16L:8D using a lamp (Osram Lumilux Daylight 860, 58 W). The average mass of the beetles was 182.94 ± 27.71 mg. Traction experiments performed in order to analyse the differences in insect adhesion with leaf

ontogenetic stage were carried out in a similar way as described in Prüm et al. 2012 [22, 23]. Maximum walking frictional forces were measured using a highly sensitive force transducer (FORT 25, force range: 0-0.25 N, World Precision Instruments Inc., Sarasota, USA) that was attached to the beetle's elytra via human hair using a tiny drop of molten beeswax. Forces were recorded for at least 2 min of active walking with ambient mean temperature of 25.0 ± 0.8 °C and humidity of 55.0 ± 5.2 % RH. Only data from straightforward walking with less than ± 2-degree variation were taken into consideration. Within each measurement, in other words the force over time curve, 15 highest local maxima with a minimum interval of 3 s between neighbouring peaks were identified and the median of these 15 maxima was extracted. The measurements were repeated with 8 different beetles on each replica. Supplementary Fig. S5 shows a schematic of experimental setup used for traction experiments and supplementary video shows a beetle walking on the replica surface.

Statistics

Statistical comparisons were performed with ANOVA on a generalized linear mixed model (GLMM) using the *R* software environment version 3.6.1 [58] and the *lme4* package [59]. Both the original and ranked data has non-normal distribution and non-homogeneity in variances. The experimental design included repeated measures and five replicates for each leaf stage. So, GLMM with gamma distribution and log link was used to test the differences in traction forces with growth stages as fixed factor, and replicates (leaf samples) and beetles as random factors. Before the comparisons one outlier adjustment on a single observation of glass (out of 40, glass) was made with rounded value of the median. For comparisons of Rc, Ra, Rsm and AR, GLMM with gamma distribution (log link) was used with replicates as random factors and leaf area as covariate. Post-hoc tests were conducted using multiple comparison of means with Tukey contrasts using the *emmeans* package [60]. Values of $p < 0.05$ were considered to be statistically significant.

The datasets generated during and/or analysed during the current study are available from the corresponding author on reasonable request.

References

1. Boege, K. & Marquis, R. J. Facing herbivory as you grow up: the ontogeny of resistance in plants. *Trends Ecol. Evol.* **20,** 441–448 (2005).

2. Barton, K. E. & Koricheva, J. The Ontogeny of Plant Defence and Herbivory: Characterizing General Patterns Using Meta-Analysis. *Am. Nat.* **175,** 481-493 (2010).

3. Barton, K. E. & Boege, K. Future directions in the ontogeny of plant defence: understanding the evolutionary causes and consequences. *Ecol. Lett.* **20,** 403-411 (2017).

4. Pearse, I. S., Harris, D. J., Karban, R. & Sih, A. Predicting novel herbivore–plant interactions. *Oikos* **122,** 1554-1564 (2013).

5. Gorb, S. N. *Attachment Devices of the Insect Cuticle*, (Kluwer Academic, 2003).

6. Gorb, E. & Gorb, S. N. Attachment ability of the beetle Chrysolina fastuosa on various plant surfaces. *Entomol. Exp. Appl.* **105,** 13-28 (2002).

7. Hanley, M. E., Lamont, B. B., Fairbanks, M. M. & Rafferty, C. M. Plant structural traits and their role in anti-herbivore defence. *Perspect. Plant Ecol.* **8,** 157–178 (2007).

8. Carmona, D., Lajeunesse, M. J. & Johnson, M. T. Plant traits that predict resistance to herbivores. *Funct. Ecol.* **25,** 358-367 (2011).

9. Gong, B. & Zhang, G. Interactions between plants and herbivores: A review of plant defence. *Acta Ecol. Sin.* **34,** 325–336 (2014).

10. Kerstiens, G. *Plant Cuticles, an Integrated Functional Approach*. (Bios Scientific, 1996).

11. Riederer, M. & Müller, C. *Biology of the Plant Cuticle*. *Annual Plant Reviews 23*. (Blackwell, 2006).

12. Kumar, C. et al. Replicating the complexity of natural surfaces: technique validation and applications for biomimetics, ecology and evolution. *Phil. Trans. R. Soc. A* **377,** 20180265; 10.1098/rsta.2018.0265 (2019).

13. Barthlott, W. & Ehler, N. *Rasterelektronenmikroskopie der Epidermisoberflächen von Spermatophyten*. (Wiesbaden: Franz-Steiner, 1977)

14. Koch, K., Bhushan, B. & Barthlott, W. Diversity of structure, morphology, and wetting of plant surfaces (invited). *Soft Matter* **4,** 1943-1963 (2008).

15. Jeffree, C. E. The Fine Structure of the Plant Cuticle in *Biology of the Plant Cuticle. Annual Plant Reviews 23* (ed. Riederer M. & Müller C.) 11-110 (Blackwell, 2006)

16. Barthlott, W., Mail, M., Bhushan, B. & Koch, K. Plant Surfaces: Structures and Functions for Biomimetic Innovations. *Nano-Micro Lett.* **9,** 23 (2017).

17. Whitney, H. M. & Federle, W. Biomechanics of plant-insect interactions. *Curr. Opin. Plant Biol.* **16,** 105–111 (2013).

18. Stork, N. E. The form of plant waxes: a means preventing insect attachment? in *Insects and the Plant Surface*. (ed. Juniper, B. E. & Southwood, T. R. E.) 346-347 (Edward Arnold, 1986).

19. Eigenbrode, S. D. & Espelie, K. E. Effects of plant epicuticular lipids on insect herbivores. *Annu. Rev. Entomol.* **40,** 171-94 (1995).

20. Federle, W., Maschwitz, U., Fiala, B., Riederer, M. & Hölldobler, B. Slippery ant-plants and skilful climbers: selection and protection of specific ant partners by epicuticular wax blooms in Macaranga (Euphorbiaceae). *Oecologia* **112,** 217–224 (1997).

21. Scholz, G. et al. Improved termite resistance of wood by wax impregnation. *Int. Biodeter. Biodegr.* **64,** 688-693 (2010).

22. Prüm, B., Seidel, R., Florian, B. H. & Speck, T. Plant surfaces with cuticular folds are slippery for beetles. *J. R. Soc. Interface* **9,** 127-135 (2012).

23. Prüm, B., Seidel, R., Florian, B. H. & Speck, T. Impact of cell shape in hierarchically structured plant surfaces on the attachment of male Colorado potato beetles (Leptinotarsa decemlineata). *Beilstein J. Nanotech.* **3,** 57-64 (2012).

24. Prüm, B., Seidel, R., Bohn, H. F., Rubach, S. & Speck, T. Plant surfaces with cuticular folds and their replicas: Influence of microstructuring and surface chemistry on the attachment of a leaf beetle. *Acta Biomater.* **9,** 6360 – 6368 (2013).

25. Rahmawan, Y., Chen, C. M. & Yang, S. Recent advances in wrinkle-based dry adhesion, *Soft Matter* **10,** 5028-5039 (2014).

26. Voigt, D., Schweikart, A., Fery, A. & Gorb, S. N. Leaf beetle attachment on wrinkles: isotropic friction on anisotropic surfaces. *J. Exp. Biol.* **215,** 1975-1982 (2012).

27. Bergmann, J. B. et al. Polymerisation-induced wrinkled surfaces with controlled topography

as slippery surfaces for insects. *Adv. Mater. Interfaces, in press* (2020).

28. Peressadko, A. G. & Gorb, S. N. *Surface profile and friction force generated by insects Andrei*. 22-23 April 2004, Hanover, Germany (Bionik, 2004).

29. Voigt, D., Schuppert, J. M., Dattinger, S. & Gorb, S. N. Sexual dimorphism in the attachment ability of the Colorado potato beetle Leptinotarsa decemlineata (Coleoptera: Chrysomelidae) to rough substrates. *J. Insect Physiol.* **54,** 765-776 (2008).

30. Al Bitar, L., Voigt, D., Zebitz, C. P. & Gorb, S. N. Attachment ability of the codling moth Cydia pomonella L. to rough substrates. *J. Insect Physiol.* **56,** 1966-72 (2010).

31. Bullock, J. M. R. & Federle, W. The effect of surface roughness on claw and adhesive hair performance in the dock beetle Gastrophysa virudula. *Insect Sci.* **18,** 298–304 (2011).

32. Priyadarshan, P. M. *Biology of Hevea Rubber* (Springer, 2017).

33. Rao, A. N. Reticulate cuticle on leaf epidermis in Hevea brasiliensis Muell. *Nature* **197,** 1125-26 (1963).

34. Dijkman, M. J. *Hevea: thirty years of research in the Far East.* (University of Miami Press, 1951)

35. Lieberei, R. *Cyanogenese und Resistenz*. Habilitationsschrift, Naturwissenschaftliche Fakultät, Technische Universität Braunschweig, Germany (1984).

36. Lieberei, R., Fock, H. P. & Biehl, B. Cyanogenesis inhibits active pathogen defence in plants: Inhibition by gaseous HCN of photosynthetic CO2-fixation and respiration in intact leaves. *Angew. Bot.* **70,** 230–238 (1996).

37. Voß, K. *Biologische Bedeutung und Aktivierbarkeit der b-D-Glycosidase in Blättern von Hevea brasiliensis (Willd.) Muell. Arg. (1865)*. PhD thesis, University of Hamburg, Germany (2001).

38. Lieberei, R. South American Leaf Blight of the Rubber Tree (Hevea spp.): New Steps in Plant Domestication using Physiological Features and Molecular Markers. *Ann. Bot.* **100,** 1125–1142 (2007).

39. Fang, Y. et al. De novo transcriptome analysis reveals distinct defence mechanisms by young and mature leaves of Hevea brasiliensis (Para Rubber Tree). *Sci. Rep.* **6,** 33151; 10.1038/srep33151 (2016).

40. Hong, L., Brown, J., Segerson, N. A., Rose, J. K. C. & Roeder, A. H. K. CUTIN SYNTHASE 2 Maintains Progressively Developing Cuticular Ridges in Arabidopsis Sepals. *Mol. Plant* **10,** 560–574 (2017).

41. Martens, P. Recherches sur la cuticule. *Protoplasma* **20,** 483–515 (1933).

42. Kourounioti, R. L. A. et al. Buckling as an origin of ordered cuticular patterns in flower petals. *J. R. Soc. Interface* **10,** 20120847; 10.1098/rsif.2012.0847 (2013).

43. Rhee, Y., Hlousek-Radojcic, A., Ponsamuel, J., Liu, D. & Post-Beittenmiller, D. Epicuticular Wax Accumulation and Fatty Acid Elongation Activities Are Induced during Leaf Development of Leeks. *Plant Physiol.* **116,** 901-911 (1998).

44. Hauke, V. & Schreiber, L. Ontogenetic and seasonal development of wax composition and cuticular transpiration of ivy (Hedera helix L.) sun and shade leaves. *Planta* **207,** 67–75 (1998).

45. Bringe, K., Schumacher, C. F. A., Schmitz-Eiberger, M., Steiner, U. & Oerke, E. C. Ontogenetic variation in chemical and physical characteristics of adaxial apple leaf surfaces. *Phytochemistry* **67,** 161-170 (2006).

46. Holloway, P. J. Surface factors affecting the wetting of leaves. *Pestic. Sci.* **1,** 156-163 (1970).

47. Jayasinghe, C. K. Pests and diseases of hevea rubber and their geographical distribution. *Bulletin of the Rubber Research Institute of Sri Lanka* **40,** 1-8 (1999).

48. Sabu, T. K. & Vinod, K. V. Food Preferences of the Rubber Plantation Litter Beetle, Luprops tristis, a Nuisance Pest in Rubber Tree Plantations. *J. Insect Sci.* **9,** 72-77 (2009a).

49. Sabu, T. K. & Vinod, K. V. Population dynamics of the rubber plantation litter beetle Luprops tristis, in relation to annual cycle of foliage phenology of its host, the para rubber tree, Hevea brasiliensis. *J. Insect Sci.* **9,** 56-66 (2009b).

50. Lieberei, R. Cyanogenesis of Hevea brasiliensis during infection with Microcyclus ulei. *J. Phytopathol.* **115,** 134–146 (1986).

51. Barton, K. E., Edwards, K. F. & Koricheva, J. Shifts in woody plant defence syndromes during leaf development. *Funct. Ecol.* **33,** 2095– 2104 (2019).

52. Wolff, J. O. & Gorb, S. N. Surface roughness effects on attachment ability of the spider Philodromus dispar (Araneae, Philodromidae). *J. Exp. Biol.* **215,** 179-184 (2012).

53. Aharoni, A. et al. The SHINE clade of AP2 domain transcription factors activates wax biosynthesis, alters cuticle properties, and confers drought tolerance when overexpressed in Arabidopsis. *Plant Cell* **16,** 2463– 2480 (2004).

54. Kumar, C., Le Houérou, V., Speck, T. & Bohn, H. F. Straightforward and precise approach to replicate complex hierarchical structures from plant surfaces onto soft matter polymer. *R. Soc. Open Sci.* **5,** 172132; 10.1098/rsos.172132 (2018).

55. Leach, R. K. *Fundamental Principles of Engineering Nanometrology*. (Elsevier, 2010).

56. Schindelin, J. et al. Fiji: an open-source platform for biological-image analysis. *Nat. Methods* **9,** 676–682 (2012).

57. Neinhuis, C. & Edelmann, H. G. Methanol as a rapid fixative for the investigation of plant surfaces by SEM. *J. Microsc.* **184,** 14-16 (1996).

58. R Core Team. *R: A Language and Environment for Statistical Computing*, R Foundation for Statistical Computing, Vienna, Austria, https://www.R-project.org (2019).

59. Bates, D., Maechler, M., Bolker, B. & Walker, S. Fitting Linear Mixed-Effects Models Using lme4. *J. Stat. Softw.* **67,** 1-48 (2015).

60. Lenth, R. *emmeans: Estimated Marginal Means, aka Least-Squares Means*. R package version 1.4.2 (2019)

Acknowledgements

We thank the gardeners of the Botanic Garden, University of Freiburg for cultivating the *Hevea brasiliensis* tree, and the engineers and technicians of the Technical Workshop of the Institute for Biology II/III for the construction of the traction force measurement device. We thank Dr. Tim Kampowski for valuable discussions on the statistical analyses. We also thank Thanuja Kanamarlapudi, wife of the first author for kindly donating her long Indian hair for beetle experiments.

Author contributions

M.T and T.S designed the study and supervised it together with G.B. Data collection, data assessment and statistical analyses were carried out by V.A.S. Data evaluation and discussion of the results was a joint effort by all authors (V.A.S., G.B., T.S. and M.T.). V.A.S contributed to the first draft of the manuscript and G.B., T.S. and M.T. improved further versions. All authors gave final approval for publication.

Competing interests

The author(s) declare no competing interests.

Funding

We acknowledge the funding from the European Union's Horizon 2020 research and innovation programme under the Marie Skłodowska-Curie grant (grant agreement No. 722842, ITN Plant-inspired Materials and Surfaces—PlaMatSu) to the authors.

Figure legends

Fig. 1: ***Leaf transition:*** The leaves from the tip of a branch of *Hevea brasiliensis* tree (height > 10m) with almost vertically sagging leaves during young stages, which gradually position themselves horizontal as they grow. The image shows (a) young leaves at stage S1, (b) leaves in transition to stage S2 with the surface progressing from shiny brown in colour to dull pale green acropetally, (c) leaves at stage S3, and (d) adult leaves (S4 and S5).

Fig. 2: ***Development of leaf and of cuticular ridges*** (a) *Hevea brasiliensis* leaves at different growth stages with colour spectrum (SpyderCHECKR 24 - SCK200, Datacolor AG Europe, Rotkreuz, Switzerland). (b-g) Corresponding CLSM images of the leaf replicas at different stages: (b) Stage 1 (c) Stage 2A (d) Stage 2B (e) Stage 3 (f) Stage 4 and (g) Stage 5. The appearance of pale green colour towards the basal region of leaf at stage 2B coincides with the appearance of microscale ridges. Both the colour and the ridges progress acropetally and further develop in the following growth stages.

Fig. 3: ***Leaf replication*** The image shows a schematic of original leaves and their negative (epoxy) and positive (PDMS) replicas. Large portion of the epoxy replicas of stages S2B (basal region of the stage 2 leaves) and S3, were fused with leaf remnants. Few tiny patches and the region very close to the base of the leaves at stages S2B and S3 were free of leaf remnants. The surfaces of the PDMS positive replicas also did not have any leaf remnants.

Fig. 4: ***Remains of plant material on replicas*** Except on very scarce patches (as shown in Fig. 2 and Fig. 3), the entire area of the epoxy replicas of leaves at stages S2B and S3 retained plant cuticular material even after KOH treatment. (a - b) CLSM pictures of the positive replicas of the leaves at stages (a) S2B and (b) S3. (c) CLSM picture of a region much closer to the base of the leaf replica at the transition stage S3 where the ridge morphology is much more similar to that of adult stages (Fig. 3).

Fig. 5: ***Ridge aspect ratio vs. leaf stage*** The boxplot shows variation in the ridge (roughness) aspect ratio for glass, flat PDMS and replicas of leaves at different leaf stages. For the stages S2B and S3 realistic aspect ratio values are given for untainted replicas from tiny patches and for the replicas from tainted moulds representing the remaining surface, which have been used for traction experiments (box plots in grey, they underestimate the aspect ratio) (see Results section).

Fig. 6: ***Insect traction forces*** The box plot shows the differences in traction forces of *Leptinotarsa decemlineata (n=40)* for a set of statistical replicates of PDMS replica surfaces of leaves at different growth stages compared with glass and flat PDMS glass replicas. The traction

force values for stage 2B and stage 3 could only be made on replicas from tainted moulds (box plots in grey) and therefore overestimate the real values (see Results section).

Fig. 7: ***Insect adhesion in interaction with plant surface:*** (a) Colorado potato beetle (*Leptinotarsa decemlineata*) walking on a leaf replica, (b) SEM image showing tarsal features on the mid leg of female Colorado potato beetle *Leptinotarsa decemlineata*, (c) SEM image showing spatula-type terminal ends of the hairy attachment system of the insect. (d - e) Schematic representation of the interfacial contact area formation between the terminal ends of insect setae and the leaf surfaces at early (d) and adult (e) growth stages of *Hevea brasiliensis* leaves.

Tables

Table 1. Median values of the roughness parameters from all the replicates of glass, flat PDMS and leaf replica surfaces. For state S2B and S3 values from untainted small areas are given representing the realistic high aspect ratio of ridges (values not in parenthesis) and values from replicas from tainted moulds underestimating the real aspect ratio (values in parenthesis) are given, which have been used in traction experiments of these two states.

Surface	***Age (days)***	***Ra (µm)***	***Rc (µm)***	***Rsm (µm)***	***Aspect ratio = Rc/Rsm***	***Rsk***
Glass	-	0.0004	0.001	1.020	0.001	0.346
Flat PDMS	-	0.0005	0.002	1.250	0.002	0.328
S1	13 ± 2	0.008	0.031	4.465	0.006	-0.906
S2A	15 ± 3	0.010	0.038	4.440	0.008	-0.768
S2B	15 ± 3	0.111 (0.044)	0.358 (0.152)	1.095 (1.465)	0.323 (0.102)	-0.265 (-0.48)
S3	16 ± 3	0.132 (0.053)	0.418 (0.173)	1.13 (1.33)	0.378 (0.129)	-0.27 (-0.495)
S4	21 ± 4	0.181	0.542	2.105	0.261	0.215
S5	> 60	0.190	0.579	2.020	0.283	0.035

Figures

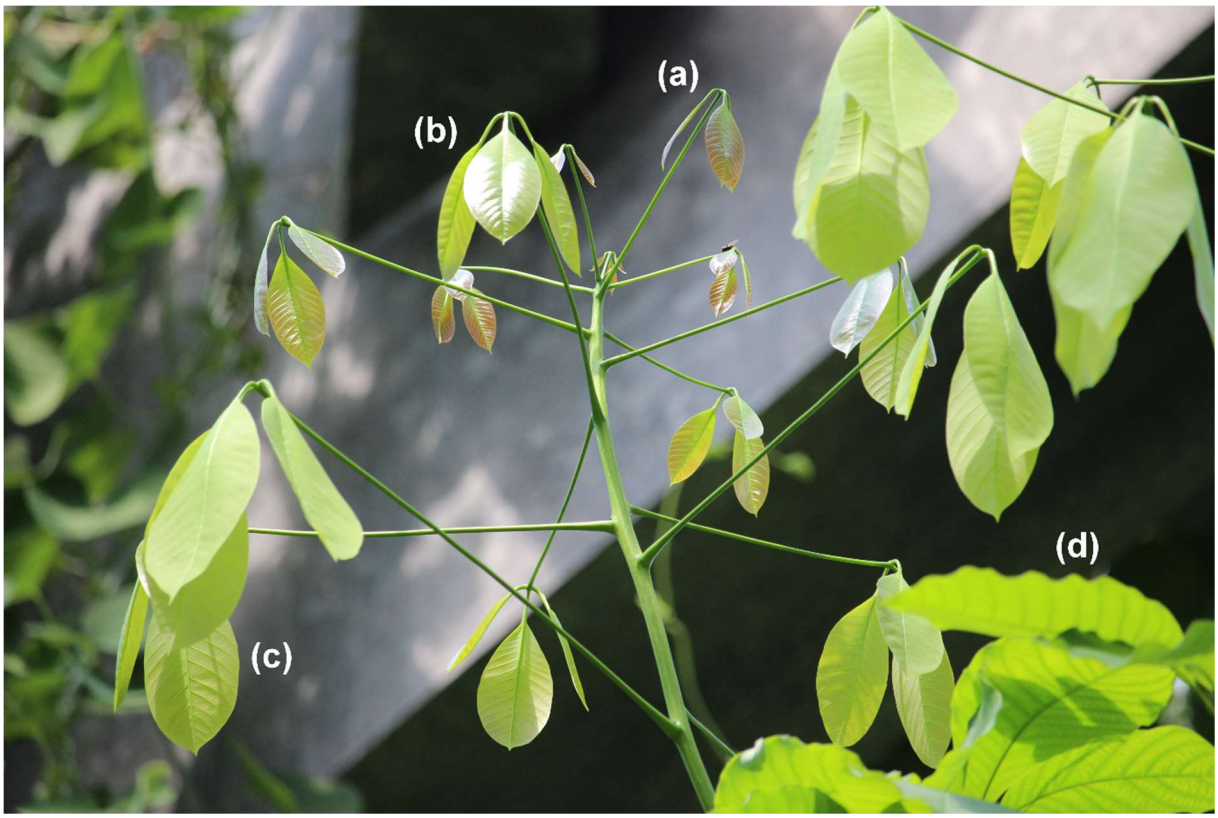

Fig. 1: ***Leaf transition:*** The leaves from the tip of a branch of *Hevea brasiliensis* tree (height > 10m) with almost vertically sagging leaves during young stages, which gradually position themselves horizontal as they grow. The image shows (a) young leaves at stage S1, (b) leaves in transition to stage S2 with the surface progressing from shiny brown in colour to dull pale green acropetally, (c) leaves at stage S3, and (d) adult leaves (S4 and S5).

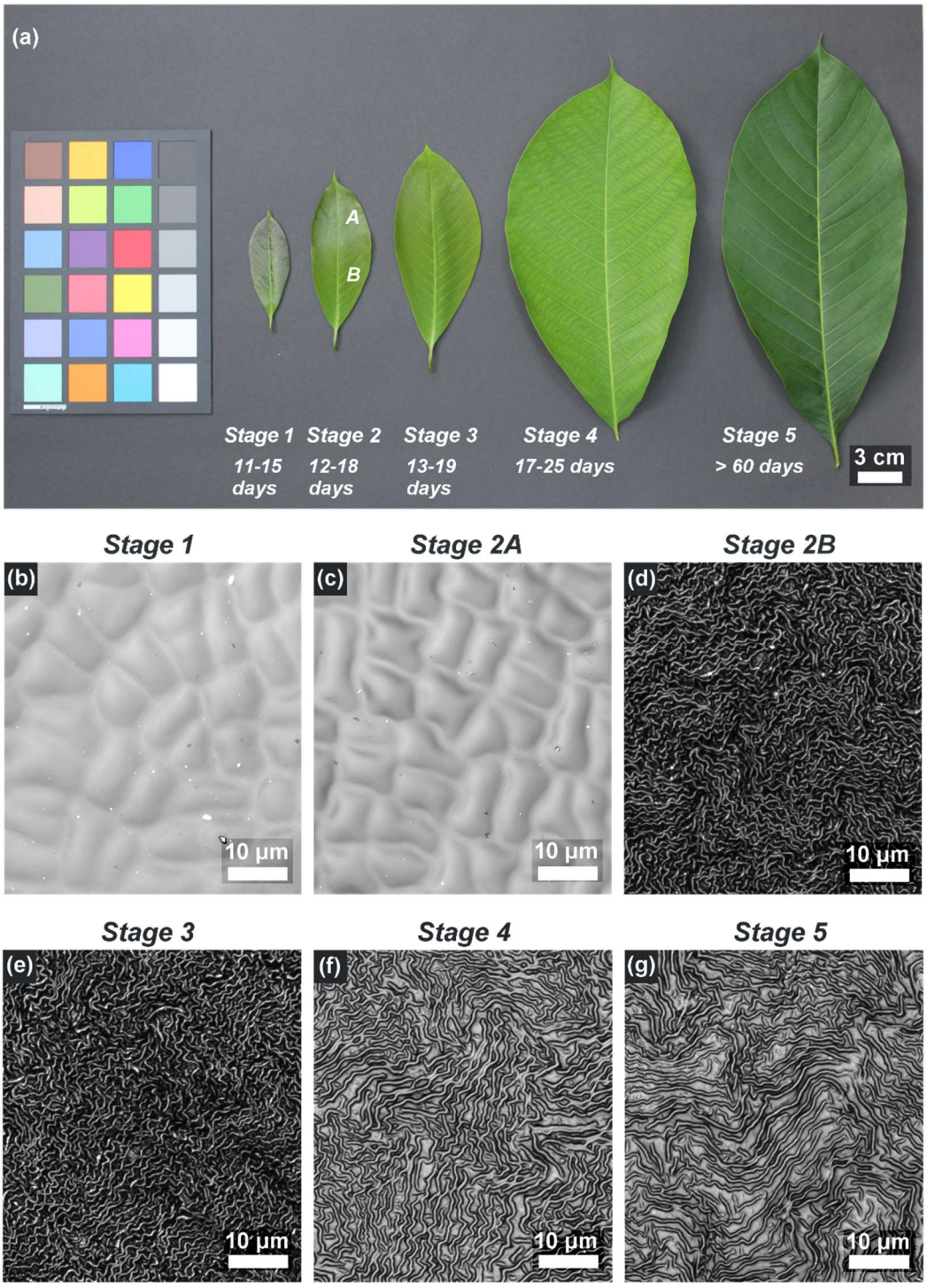

Fig. 2: ***Development of leaf and of cuticular ridges*** (a) *Hevea brasiliensis* leaves at different growth stages with colour spectrum (SpyderCHECKR 24 - SCK200, Datacolor AG Europe, Rotkreuz, Switzerland). (b-g) Corresponding CLSM images of the leaf replicas at different stages: (b) Stage 1 (c) Stage 2A (d) Stage 2B (e) Stage 3 (f) Stage 4 and (g) Stage 5. The appearance of pale green colour towards the basal region of leaf at stage 2B coincides with the appearance of microscale ridges. Both the colour and the ridges progress acropetally and further develop in the following growth stages.

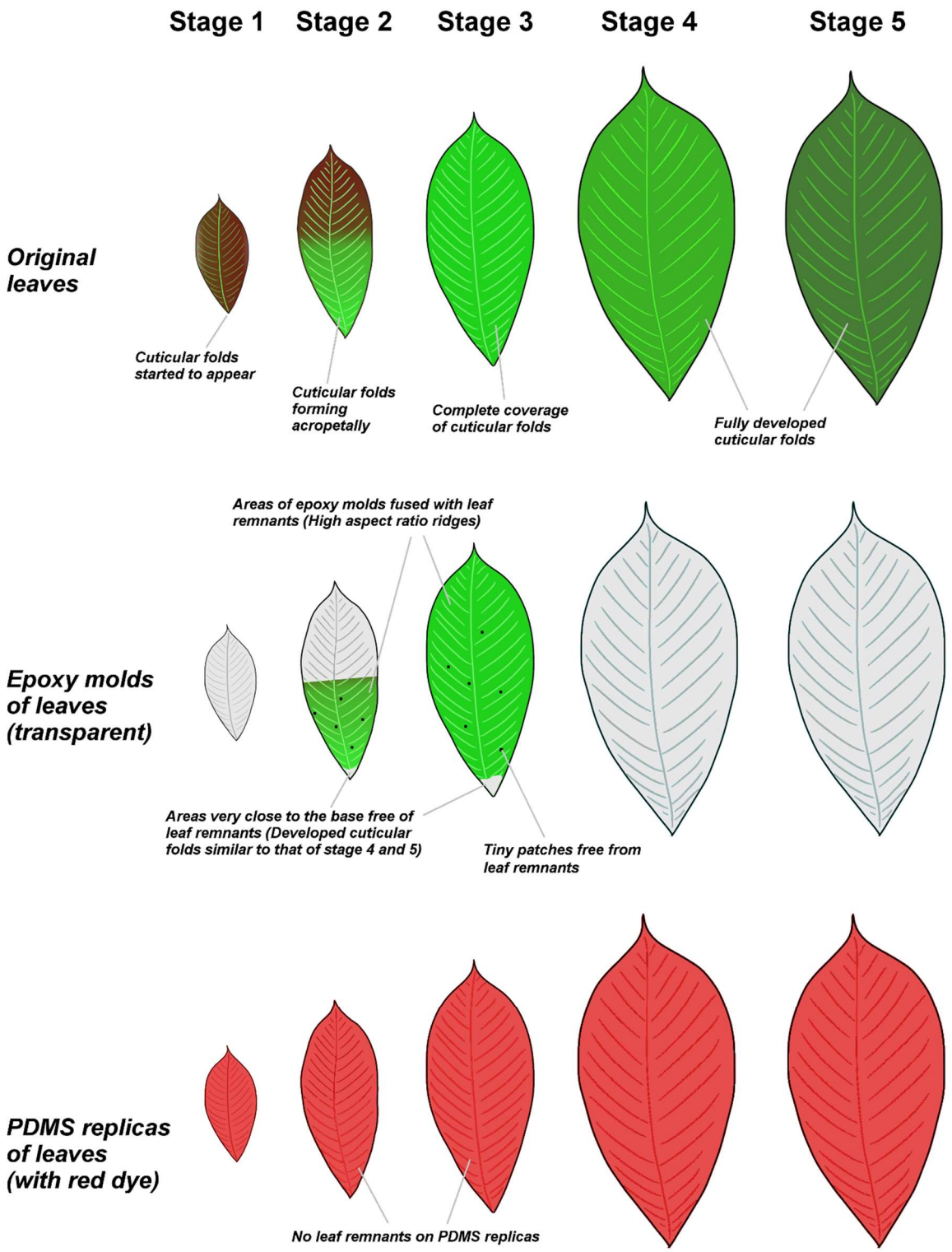

Fig. 3: ***Leaf replication*** The image shows a schematic of original leaves and their negative (epoxy) and positive (PDMS) replicas. Large portion of the epoxy replicas of stages S2B (basal region of the stage 2 leaves) and S3, were fused with leaf remnants. Few tiny patches and the region very close to the base of the leaves at stages S2B and S3 were free of leaf remnants. The surfaces of the PDMS positive replicas also did not have any leaf remnants.

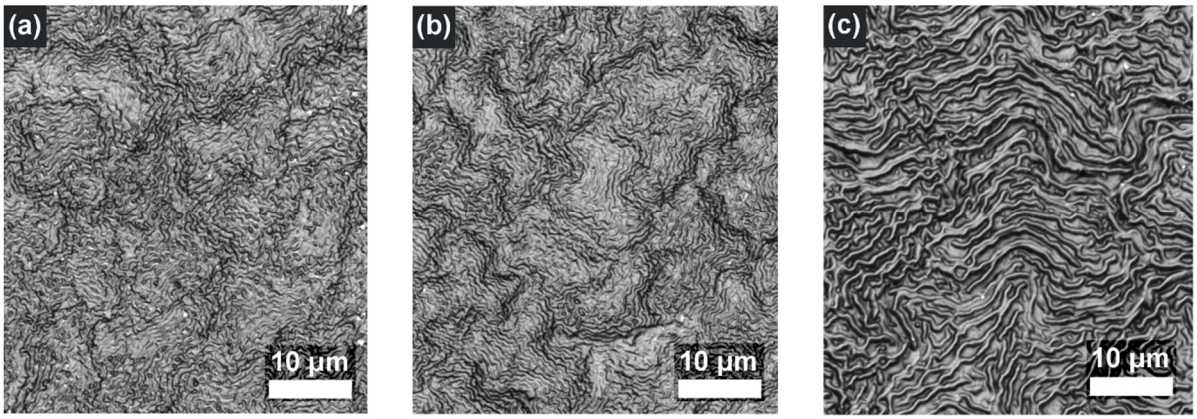

Fig. 4: ***Remains of plant material on replicas*** Except on very scarce patches (as shown in Fig. 2 and Fig. 3), the entire area of the epoxy replicas of leaves at stages S2B and S3 retained plant cuticular material even after KOH treatment. (a-b) CLSM pictures of the positive replicas of the leaves at stages (a) S2B and (b) S3. (c) CLSM picture of a region much closer to the base of the leaf replica at the transition stage S3 where the ridge morphology is much more similar to that of adult stages (Fig. 3).

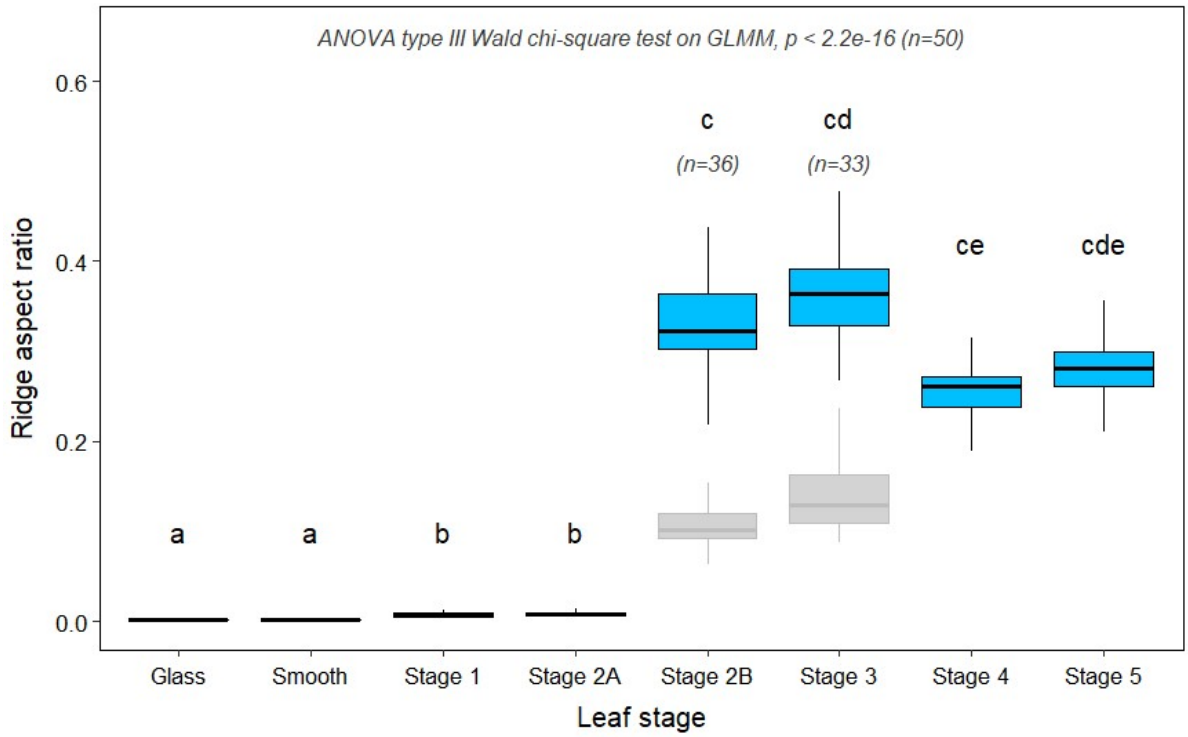

Fig. 5: ***Ridge aspect ratio vs. leaf stage*** The boxplot shows variation in the ridge (roughness) aspect ratio for glass, flat PDMS and replicas of leaves at different leaf stages. For the stages S2B and S3 realistic aspect ratio values are given for untainted replicas from tiny patches and for the replicas from tainted moulds representing the remaining surface, which have been used for traction experiments (box plots in grey, they underestimate the aspect ratio) (see Results section).

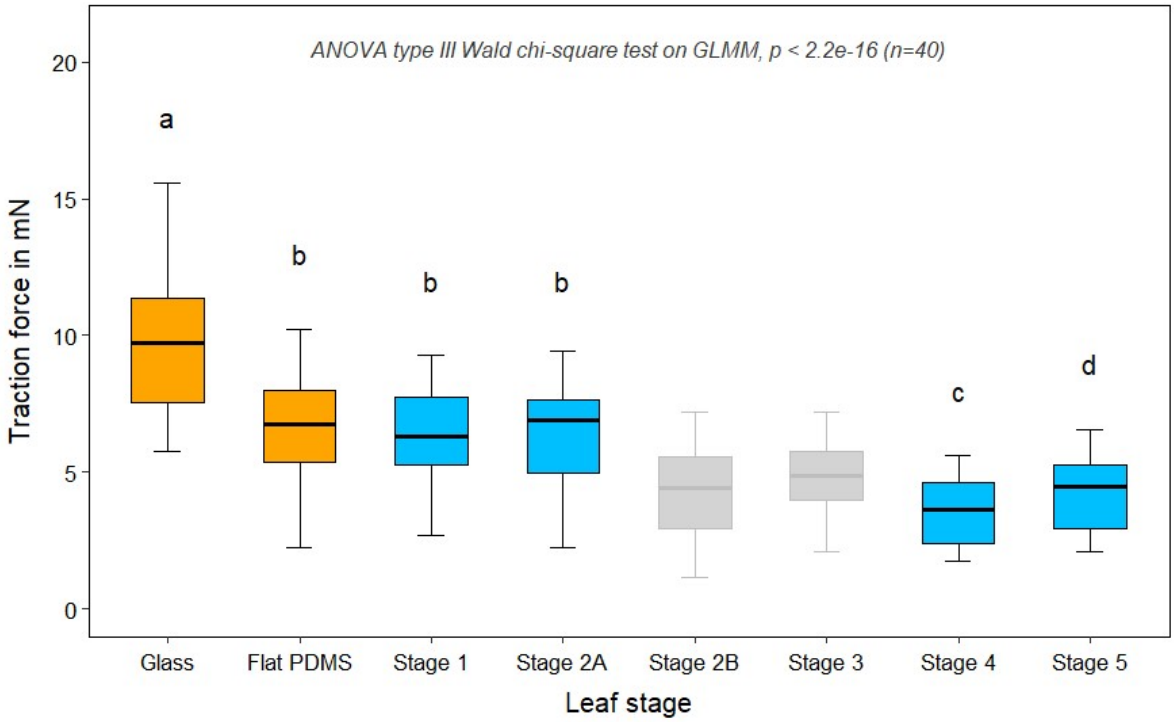

Fig. 6: ***Insect traction forces*** The box plot shows the differences in traction forces of *Leptinotarsa decemlineata (n=40)* for a set of statistical replicates of PDMS replica surfaces of leaves at different growth stages compared with glass and flat PDMS glass replicas. The traction force values for stage 2B and stage 3 could only be made on replicas from tainted moulds (box plots in grey) and therefore overestimate the real values (see Results section).

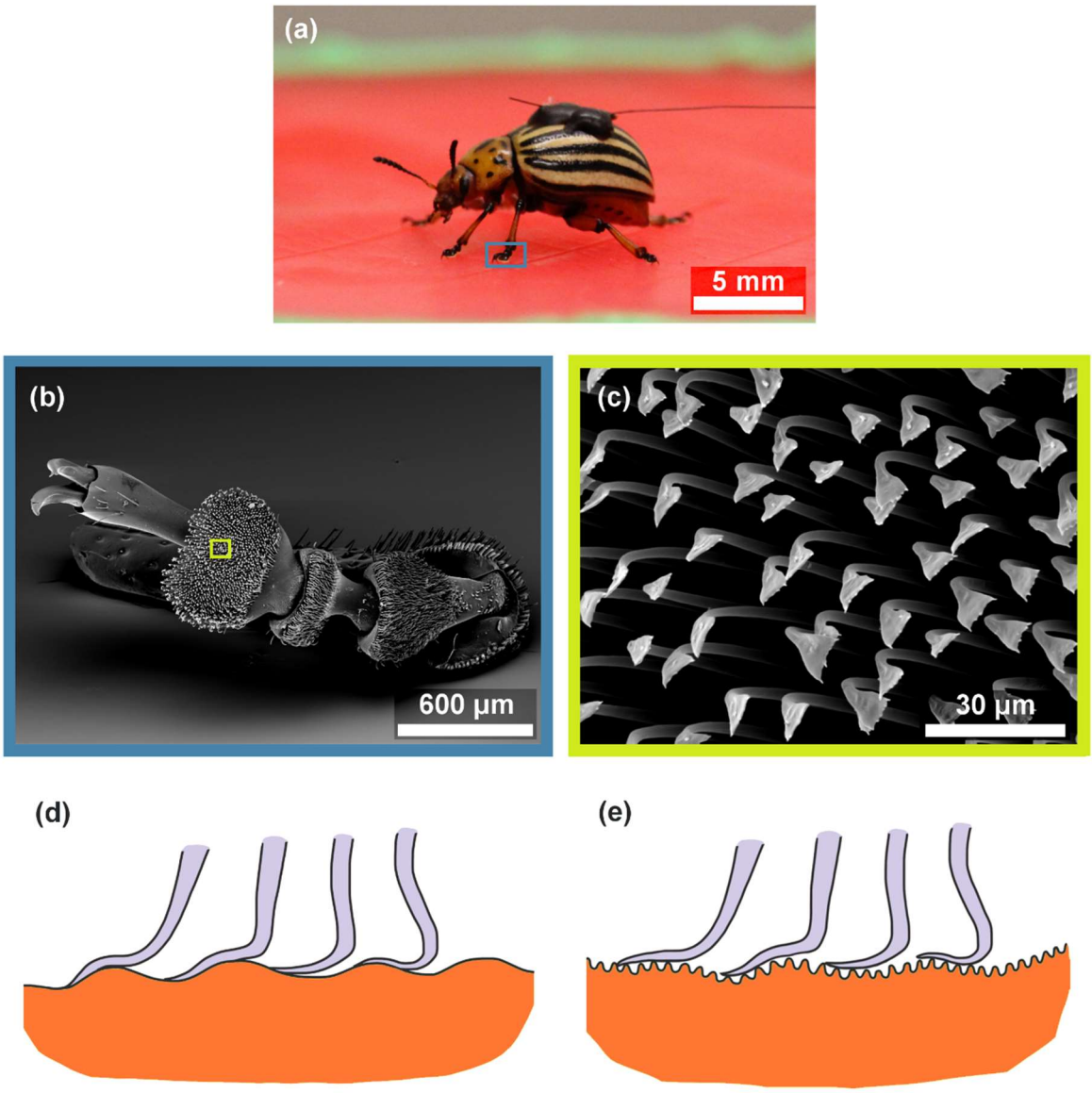

Fig. 7: ***Insect adhesion in interaction with plant surface:*** (a) Colorado potato beetle (*Leptinotarsa decemlineata*) walking on a leaf replica, (b) SEM image showing tarsal features on the mid leg of female Colorado potato beetle *Leptinotarsa decemlineata*, (c) SEM image showing spatula-type terminal ends of the hairy attachment system of the insect. (d – e) Schematic representation of the interfacial contact area formation between the terminal ends of insect setae and the leaf surfaces at early (d) and adult (e) growth stages of *Hevea brasiliensis* leaves.